P2.1.6

VERIFICATION OF ION IMPLANTATION MODELS BY MONTE CARLO SIMULATIONS

G. Hobler, S. Selberherr

Institut für Allgemeine Elektrotechnik und Elektronik
Technical University of Vienna
Gußhausstraße 27-29, A-1040 Vienna, AUSTRIA

Monte Carlo simulations are perfectly suited to check the validity of simple models. We investigate 3 models: First, we show that 1D models for the implantation into multilayer targets give reasonable results only if the stopping powers of mask and bulk material are similar. Second, we discuss the construction of 2D point responses from 1D profiles. Third, we show that the method of superposing point responses at mask edges may fail in some cases.

1. INTRODUCTION

The Monte Carlo method is known to be the most powerful tool for the simulation of ion implantation. Analytical models, however, require much less CPU times and allow easy consideration of experimental data. The latter is particularly important because Monte Carlo simulations usually assume amorphous targets so that they do not always yield correct profiles for implantations into crystalline targets [1].

As simple models are usually based on physical considerations and Monte Carlo simulations take physics most accurately into account (apart from the assumption of amorphous targets), Monte Carlo simulations are perfectly suited to check the validity of these simple models. In particular, we will investigate in this paper 1D models for the implantation into multilayer targets (Chapter 2), the construction of 2D point responses from 1D profiles (Chapter 3), and the method of superposing point responses to obtain dopant distributions near mask edges (Chapter 4).

Our Monte Carlo program is, from a physical point of view, similar to the well known program TRIM [2]. One mayor difference of our code is that we evaluate scattering angles by interpolation in a precomputed table. The 2D simulations have been performed with a code which allows arbitrary geometries. Both features are described in Ref. [3].

2. IMPLANTATION INTO MULTILAYER TARGETS

In a recent paper [4], Ryssel discussed 5 models for the implantation into multilayer targets. These models consider 3 situations:

1) Implantation into bare material 1 (concentration profile $C_1(x)$).
2) Implantation into bare material 2 (concentration profile $C_2(x)$).
3) Implantation into a mask/bulk structure with given mask thickness d, where the mask material is material 1 and the bulk material is material 2 (concentration profile $C(x)$).

The purpose of the models is to construct $C(x)$ from $C_1(x)$ and/or $C_2(x)$. $C_1(x)$ and $C_2(x)$ may be obtained by simulations as well as by experiments. The models read:

$$C(x) = \begin{cases} C_1(x) & x < d \\ \alpha \cdot C_2\left(x - d \cdot \left(1 - \frac{R_{p2}}{R_{p1}}\right)\right) & x > d \end{cases} \tag{1}$$

$$C(x) = \begin{cases} C_1(x) & x < d \\ C_2\left(x - \left(d - d'\right)\right) & x > d \end{cases} \tag{2}$$

$$C(x) = \begin{cases} \frac{R_{p2}}{R_{p1}} \cdot C_2\left(\frac{R_{p2}}{R_{p1}} \cdot x\right) & x < d \\ C_2\left(x - d \cdot \left(1 - \frac{R_{p2}}{R_{p1}}\right)\right) & x > d \end{cases} \tag{3}$$

$$C(x) = \begin{cases} \frac{\Delta R_{p2}}{\Delta R_{p1}} \cdot C_2\left(\frac{\Delta R_{p2}}{\Delta R_{p1}} \cdot x\right) & x < d \\ C_2\left(x - d \cdot \left(1 - \frac{\Delta R_{p2}}{\Delta R_{p1}}\right)\right) & x > d \end{cases} \tag{4}$$

$$C(x) = \begin{cases} C_1(x) & x < d \\ \frac{\Delta R_{p1}}{\Delta R_{p2}} \cdot C_1\left(\frac{\Delta R_{p1}}{\Delta R_{p2}} \cdot x - d \cdot \left(\frac{\Delta R_{p1}}{\Delta R_{p2}} - 1\right)\right) & x > d \end{cases} \tag{5}$$

α in (1) and d' in (2) are adjusted in such a way that $\int C(x)dx = \int C_1(x)dx$ ($= \int C_2(x)dx$), what is automatically fulfilled in Models 3, 4, and 5. R_{p1}, R_{p2} denote the mean projected range and ΔR_{p1}, ΔR_{p2} the standard deviation of $C_1(x)$, $C_2(x)$.

Ryssel gave qualitative arguments in favour of Model 1. To investigate the models quantitatively, we have calculated $C_1(x)$, $C_2(x)$ and $C(x)$ by Monte Carlo simulations and then constructed $C(x)$ from $C_1(x)$ and $C_2(x)$ by applying one of the Models 1-5. Comparing the two versions of $C(x)$, one can easily see how good the models are.

Two examples are shown in Fig.1 and Fig.2. Fig.1 shows good agreement between Model 1 and Monte Carlo results for an As-implantation into SiO_2/Si. In Fig.2 can be seen, however, that the model fails completely for a Be- implantation into SiO_2/GaAs. In this case the profile in bare SiO_2 would describe the profile in SiO_2/GaAs much better than the profile constructed by Model 1. This indicates that the models fail, if mask and bulk material have very different stopping powers like SiO_2 and GaAs.

To confirm this result, we have performed simulations for B-, As-, Sb-, and Be-, Si-, Zn- implantations into SiO_2/Si and SiO_2/GaAs, respectively, at 3 different energies and for 3 values of the mask thickness. P-implantations have not been considered because P-profiles in SiO_2 and Si are almost identical. The energies are usually 30 keV, 100 keV, and 500 keV (10, 80, 500 for B and Be), the values for the mask thickness about $\frac{1}{5}R_p$ ("thin"), $\frac{4}{5}R_p$ ("medium"), $\frac{7}{5}R_p$ ("thick"). In order to present the results in a compact manner, we have introduced 4 degrees (cf. Tab.1 and Tab.2): "good" means that the profiles deviate in depth far less than 10%, "fair" means less than 10%, "poor" more than 10%. "catastrophic" has been introduced to indicate that one of $C_1(x)$, $C_2(x)$ would represent the profile in the mask/bulk structure better than $C(x)$ as calculated from the model.

In Tab.1 and Tab.2 there is listed for each mask thickness and each model the number of cases with good, fair, poor, and catastrophic agreement. (Note that the sum of each column is 9, as we have 3 ion species at 3 energies). In Tab.1, which is for SiO_2/Si, it can be seen that the general agreement is quite good, however, only Models 1 and 3 are always "good" or "fair", and Model 1 is slightly better than Model 3, in agreement with Ryssel [4]. On the other hand, all models completely fail for SiO_2/GaAs (Tab.2). Only for thin masks Model 3 gives good results.

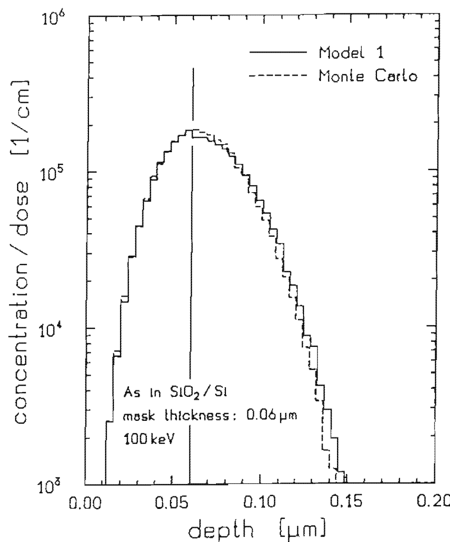

FIGURE 1

As-implantation into Si through a SiO_2 mask.
dashed line: Monte Carlo profile in SiO_2/Si.
full line: Profile in SiO_2/Si due to Model 1, constructed from Monte Carlo profiles in bare SiO_2 and bare Si.

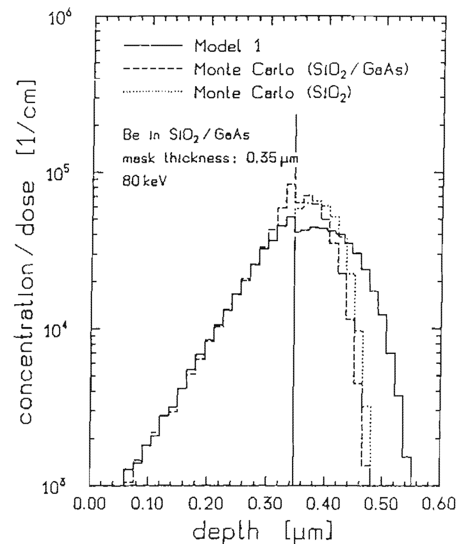

FIGURE 2

Be-implantation into GaAs through a SiO_2 mask.
dashed line: Monte Carlo profile in SiO_2/GaAs.
full line: Profile in SiO_2/GaAs due to Model 1, constructed from Monte Carlo profiles in bare SiO_2 and bare GaAs.
dotted line: Monte Carlo profile in bare SiO_2.

mask	thin					medium					thick				
model	1	2	3	4	5	1	2	3	4	5	1	2	3	4	5
good	9	4	9	7	1	6	5	5	3	5	9	9	4	1	9
fair	-	3	-	2	2	3	4	4	1	4	-	-	5	2	-
poor	-	1	-	-	6	-	-	-	5	-	-	-	-	6	-
catastrophic	-	1	-	-	-	-	-	-	-	-	-	-	-	-	-

TABLE 1

Number of cases with good, fair, poor, and catastrophic agreement for implantations into SiO_2/Si.

mask	thin					medium					thick				
model	1	2	3	4	5	1	2	3	4	5	1	2	3	4	5
good	3	-	6	2	-	-	-	-	-	-	-	-	-	-	-
fair	2	-	2	-	-	3	-	1	-	-	-	-	-	-	-
poor	-	2	-	3	-	3	1	3	1	1	1	1	1	-	-
catastrophic	4	7	1	4	9	3	8	5	8	8	8	8	8	9	9

TABLE 2

Number of cases with good, fair, poor, and catastrophic agreement for implantations into $SiO_2/GaAs$.

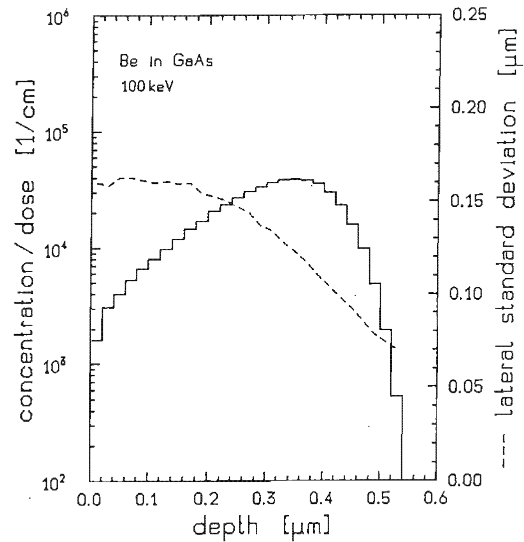

FIGURE 3

Depth dependence of the lateral standard deviation for Be in GaAs (100 keV).

3. CONSTRUCTION OF POINT RESPONSES FROM 1D PROFILES

Responses to punctiform beams play an important role in the Superposition Method (see Chapter 4). For a long time it was believed that one parameter, namely the lateral standard deviation, would be enough information to construct the 2D point response $C(x,y)$ from the 1D profile $C_{vert}(x)$. This was simply done by multiplying $C_{vert}(x)$ with the lateral Gaussian function $gauss(y)$ given by σ_y:

$$C(x,y) = C_{vert}(x) \cdot gauss(y) \qquad (6)$$

This means that the lateral profile at any depth is a Gaussian function with fixed standard deviation. In a previous paper [5] we have shown that this is not true for Si-targets. The lateral standard deviation depends strongly on the depth, and also the lateral profile is not always well represented by a Gaussian function.

We have now investigated GaAs-targets, and we found quite the same behaviour as for Si: For light ions (Be) the lateral standard deviation decreases with depth (Fig.3) and the lateral kurtosis is smaller than 3. For heavy ions (Zn) the standard deviation increases with depth and the kurtosis may assume large values near the surface. For Si-ions, which lie between the two cases, σ_y does not depend very much on the depth.

4. SUPERPOSITION METHOD

The superposition law says that the response to a homogenous beam is identical to the sum of responses to punctiform beams which are equidistributed over the width of the homogenous beam. For a rigorous application of this law we would have to know the actual response to every punctiform beam along the surface. In practice, however, point responses are constructed from 1D profiles and may therefore not take into account boundaries other than perpendicular to the beam. In the case of a mask edge those ions are not treated correctly by the superposition method which leave the mask laterally and re-enter the target. The question is now, whether these ions may significantly contribute to the total dopant concentration.

To investigate this question, we have performed Monte Carlo simulations for a simple structure, namely a rectangular mask on a planar bulk. In this case, according to the superposition method, no ions should reach the Si-region which have originally entered the mask. So, if we only expose the mask surface to the computational ion beam, any concentration in the Si-region indicates a failure of the model. We have performed simulations for B- and As-implantations at various energies. The results for B at 100 keV are shown in Fig.4. The concentration in Si is about one order of magnitude lower than the peek concentration of di-

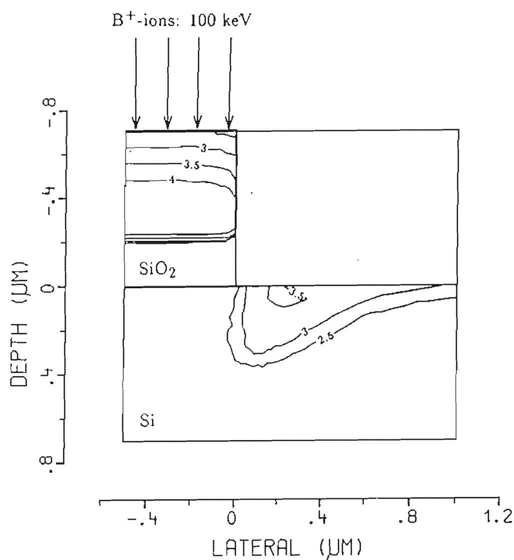

FIGURE 4

B-implantation into Si by a rectangular mask.
The contour lines represent the logarithm of the dopant concentration devided by the dose |1/cm|.
Only the mask region is exposed to the beam.

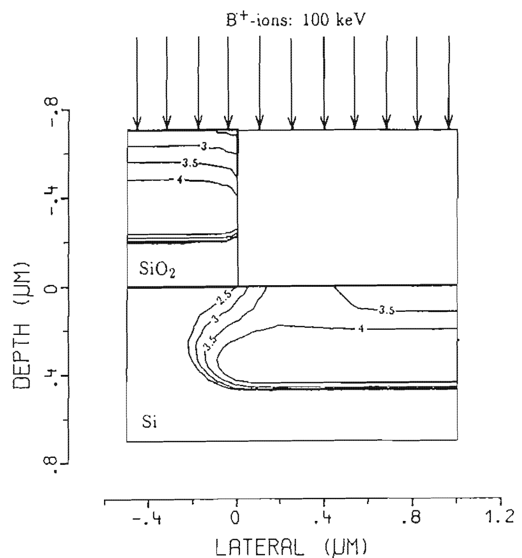

FIGURE 5

B-implantation into Si by a rectangular mask.
The contour lines represent the logarithm of the dopant concentration devided by the dose |1/cm|.
The whole simulation area is exposed to the beam.

rectly implanted ions. This is typical for all cases we have simulated.

In Fig.5 it can be seen that this extra concentration —as compared with what is expected by the superposition method—contributes significantly to the total distribution. According to the superposition method, the contour lines labeled by "3.5" and "4" should be straight lines for lateral coordinates from slightly larger than 0 up to 1. Also the contour line labeled by "3" should be seen there.

For As- and low energy B-implantations this extra concentration may be well neglected, because in these cases the profiles have their maximum near the surface and will therefore cover the dopants which have made their way through the mask. A similar situation as in Fig.4 and Fig.5 is expected for high-energy P-implantations.

To avoid this effect, one could use a thicker mask, since the ions which leave the mask laterally will then spread over a wider range. E.g., for a mask thickness of $2\mu m$ in Fig.5 the effect would almost disappear. Another possibility would be to tilt the mask edge. In this case, however, the dopant distribution below the mask edge would be increased.

ACKNOWLEDGEMENTS

This work has been supported by the research laboratories of SIEMENS AG at Munich, by DIGITAL EQUIPMENT CORP. at Hudson, USA, and by the "Fonds zur Förderung der wissenschaftlichen Forschung", project S43/10.

REFERENCES

|1| H. Ryssel, J.P. Biersack:
"Ion Implantation Models for Process Simulation", In: *Process and Device Modeling* (Ed. W.L. Engl), Elsevier, North Holland, pp. 31–69, 1986.

|2| J.P. Biersack, L.G. Haggmark:
"A Monte Carlo Computer Program for the Transport of Energetic Ions in Amorphous Targets" *Nucl. Instr. Meth.*, Vol. 174, pp. 257–269, 1980.

|3| G. Hobler, S. Selberherr:
"Efficient Two-Dimensional Monte Carlo Simulation of Ion Implantation" *Proc. NASECODE V Conf.*, Dublin, 1987.

|4| H. Ryssel, J. Lorenz, K. Hoffmann:
"Models for Implantation into Multilayer Targets" *Appl. Phys.*, Vol. A41, pp. 201–207, 1986.

|5| G. Hobler, E. Langer, S. Selberherr:
"Two-Dimensional Modeling of Ion Implantation with Spatial Moments" *Sol.-State Electron.*, Vol. 30, No. 4, pp. 445–455, 1987.